J. Phys. B: At. Mol. Opt. Phys. 28 (1995) 3047–3062. Printed in the UK

Mixed gauge approach to multiphoton wavefunctions

F Robicheaux, C-T Chen, P Gavras and M S Pindzola
Department of Physics, Auburn University, Auburn, AL 36849, USA

Received 6 February 1995, in final form 3 April 1995

Abstract. We present a novel method for obtaining Floquet or time-dependent wavefunctions for atoms in laser fields. This method has the potential to be more stable and/or faster than previous methods. The main idea is to include the effects of the laser field in a gauge that smoothly changes character as a function of distance. This transformation allows us to formally account for the analytic behaviour of the wavefunction as $r \rightarrow \infty$ and as $r \rightarrow 0$. We demonstrate the feasibility of this mixed gauge approach through Floquet calculations on a one-dimensional model problem and three-dimensional calculations for the hydrogen atom. Time-dependent calculations for a one-dimensional model problem are performed with the mixed gauge. This approach may also be useful for exploring analytic and perturbative properties of the wavefunction in the high-field limit.

1. Introduction

There have been many different theoretical methods used for describing the interaction of an electron with a static potential and a strong laser field (i.e. the laser field has a non-perturbative effect on the electronic motion). The different methods can be generically grouped into two classes: time-dependent and Floquet methods. The time-dependent methods directly solve the time-dependent Schrödinger equation for a laser pulse with a time-dependent intensity (for example, Kulander 1988, Krause *et al* 1992, Xu *et al* 1992, Schwengelbeck and Faisal 1994, Pindzola and Bottcher 1993, Collins and Merts 1989, LaGattuta 1991, Grobe and Eberly 1993). The Floquet wavefunctions assume a constant (or slowly varying) laser intensity; this type of wavefunction can be obtained by several methods: expansion in an L^2 basis (Maquet *et al* 1983, Potvliege and Shakeshaft 1989, Madajczyk *et al* 1992, Potvliege and Smith 1993, and Dörr *et al* 1994), analytic solution of Schrödinger's equation (Pont *et al* 1990, 1992), direct solution of the close-coupling equations (Dimou and Faisal 1994, Giusti-Suzor and Zoller 1987, Marte and Zoller 1991, Collins and Csanak 1991), or by the R-matrix method (Burke *et al* 1990, Dörr *et al* 1992). All of these theoretical techniques have used the 'pure' gauges for the electromagnetic field in order to obtain the wavefunction (i.e. length gauge, velocity gauge, or 'acceleration gauge'). It is probable that these gauges are favoured because the resulting Hamiltonian for the electron is very simple. In this paper, we would like to draw attention to the obvious fact that there exist an infinite number of gauges and that the gauge can be chosen in order to make the wavefunction simple (instead of the Hamiltonian simple).

The problem of obtaining a Floquet wavefunction to represent an atom in a monochromatic laser field does not have an easy solution. The difficulty relates to the nature of the laser–atom interaction which can have different forms depending on the gauge used to generate the scalar and vector potential. In the length gauge, the interaction diverges

0953-4075/95/143047+16$19.50

at large distances but is small at small distances. In the velocity gauge, the interaction is finite and non-zero for all distances. In the 'acceleration gauge', the interaction has the form $V(r-\alpha(t))-V(r)$ (with V being the electronic potential and $\alpha(t)$ being the oscillations of a free classical electron in the laser field) which converges to zero at large distances but gives problems at small distances for Coulomb potentials. Most dynamical situations facing atomic theorists involve finite potentials that only couple atomic degrees of freedom over a limited region of space and therefore involve channels that decouple at large distances. The short-range nature of atomic couplings has encouraged a specialization of theoretical techniques that take advantage of this fact. The exploration of atomic dynamics in a laser field using scattering theory techniques has been hampered by the non-standard nature of the laser–atom interaction.

The difficulty in constructing atomic scattering functions in the presence of a laser field can be traced to the form of the electron–laser field interaction. Only in the acceleration gauge is it possible to obtain scattering wavefunctions and several authors have used this gauge for all space. However, the acceleration gauge interaction has difficulties near $r=0$ for Coulomb potentials because of the time dependence of the singularity; it is difficult to get converged results when the acceleration gauge is used for all space except for non-Coulombic potentials or high angular momentum states where the electron cannot penetrate into the strong interaction region. Burke *et al* (1991) and Dörr *et al* (1992) have taken advantage of the nature of the laser–atom interaction to obtain Floquet wavefunctions in the length gauge near the nucleus, the velocity gauge at intermediate distances, and the acceleration gauge at large distances. The total wavefunction was obtained by matching the wavefunctions in the different regions (and therefore with different gauges) at the boundaries.

The time-dependent methods do not have obvious problems in obtaining wavefunctions in the different gauges; the electronic wavefunction is calculated time-dependently on a spatial grid of points and the electron does not get to very large distances before the laser pulse is turned off. However, it has been noticed that the length gauge cannot be used for very high intensities because at large r (where the laser interaction is largest) the de Broglie wavelength of the electron becomes too small for the spatial grid which can cause errors in the calculation. This problem can be overcome by using the velocity gauge, but some parameters (e.g. the autocorrelation function $|\langle\psi(x,t)|\psi(x,0)\rangle|^2$) may oscillate much more strongly in the velocity gauge than in the length gauge.

In this paper, we present a method for obtaining Floquet wavefunctions in a mixture of gauges. This approach is based on a general gauge transformation that approaches the length gauge at small distances, the velocity gauge at intermediate distances and the acceleration gauge at large distances. Unlike Burke *et al* (1991) and Dörr *et al* (1992), the change from one gauge to the next is accomplished smoothly over a range of distances and the transformation can be used in time-dependent calculations. This smooth evolution of the gauge has the advantage that the resulting wavefunction needs very few Floquet blocks for convergence because a part of the electron–laser interaction is included analytically in the wavefunction. The disadvantage of the method is that the resulting mixed gauge Hamiltonian is much more complicated than the length gauge Hamiltonian, velocity gauge Hamiltonian, or acceleration gauge Hamiltonian. However, in some sense this disadvantage does not present as many difficulties as the 'pure' gauges because it is the complicated nature of the wavefunction that is the main difficulty. The numerical part of the wavefunction for the mixed gauge is simpler than for the standard gauges. By using a mixed gauge, the interaction with the laser field is finite everywhere and goes to zero at $r=0$ and $r=\infty$; more of the effect of the laser field is analytically included in the wavefunction with the mixed gauge than any of the pure gauges.

The purpose of this paper is to describe how this method works and to investigate the properties of the mixed gauge procedure (e.g. convergence). For this purpose, we restrict ourselves to problems that are simple or that have already been explored in order to investigate the accuracy of the method.

2. General formulation

The wavefunction is a solution of

$$\left[\tfrac{1}{2}(\boldsymbol{p}+\boldsymbol{A}(t)/c)^2+V(\boldsymbol{r})\right]\Psi(\boldsymbol{r},t)=H\Psi(\boldsymbol{r},t)=\mathrm{i}\frac{\partial}{\partial t}\Psi(\boldsymbol{r},t) \tag{1}$$

where $V(\boldsymbol{r})$ is a static potential for the electron, $\boldsymbol{p}$ is the electron's momentum operator, and for the Floquet calculations $\boldsymbol{A}(t)=\boldsymbol{A}_0\sin(\omega t)$ with ω the frequency of the laser field for the Floquet calculations. Atomic units are used throughout this paper. We will look for wavefunctions that have the form

$$\Psi_{Ej}(\boldsymbol{r},t)=\left[\exp(-\mathrm{i}Et-\mathrm{i}\int^t \mathrm{d}t'\,\boldsymbol{A}(t')\cdot\boldsymbol{A}(t')/2c^2)\right]\mathrm{e}^{-\mathrm{i}\phi(\boldsymbol{r},\boldsymbol{p},t)}\psi_{Ej}(\boldsymbol{r},t) \tag{2}$$

where one possible choice of the phase operator is given by

$$\phi(\boldsymbol{r},\boldsymbol{p},t)=F(\boldsymbol{r})\boldsymbol{A}(t)\cdot\boldsymbol{r}/c-[G(\boldsymbol{r})\boldsymbol{A}_0\cdot\boldsymbol{p}+\boldsymbol{A}_0\cdot\boldsymbol{p}G(\boldsymbol{r})]\cos(\omega t)/2c\omega \tag{3}$$

and $F(\boldsymbol{r})$ and $G(\boldsymbol{r})$ are arbitrary functions that will be chosen for convenience. The $\boldsymbol{A}^2$ term in (2) accounts exactly for the effects of the $\boldsymbol{A}^2$ term in (1). We have chosen the form of (3) by taking the usual velocity-to-length transformation and multiplying it by a function that goes to zero at large distances (i.e. it 'turns off' the transformation at large distances) and by taking the usual velocity-to-acceleration transformation and symmetrically multiplying it by a function that goes to zero at small distances. The choice $F=1$ and $G=0$ gives the velocity-to-length gauge transformation; the choice $F=0$ and $G=1$ gives the velocity-to-acceleration gauge transformation. We will always choose F and G to be functions of $\boldsymbol{r}$ such that $F(\boldsymbol{r})G(\boldsymbol{r})=0$. This condition on F and G gives

$$\left[\phi,\frac{\partial\phi}{\partial t}\right]=0 \tag{4}$$

which will greatly simplify later equations. This constraint on F and G leaves an infinite range of possible forms for these functions. As a general procedure, F and G should (probably) be functions of r when spherical coordinates are being used in the calculation; the phase operator will then only connect states ℓ to those with $\ell\pm1$. The functions F and G should probably be functions of $r^2=\boldsymbol{r}\cdot\boldsymbol{r}$ in order to alleviate cusp problems near $r=0$ and G should go to zero faster than r^2 as r goes to zero in order to avoid singular interactions near the origin. For example, $F(\boldsymbol{r})=\exp(-\beta r^2)$ and $G=0$ gives a gauge that approaches the length gauge near the origin and velocity gauge as $r\to\infty$. As another example, the choice $F=0$ and $G(\boldsymbol{r})=1-\exp(-\beta r^4)$ gives a 'gauge' that looks like the velocity gauge near the origin and the acceleration gauge as $r\to\infty$. When cylindrical coordinates are used with light linearly polarized in the z-direction, the best choices of F and G are those where the functions only depend on z^2 (e.g. $F=\exp(-\beta z^4)$ might be a good choice).

The phase operator, as defined in (3), is a Hermitian operator which means, $\exp(-\mathrm{i}\phi)$, is a unitary operator. This property guarantees the Hermiticity of $\mathrm{e}^{\mathrm{i}\phi}H\mathrm{e}^{-\mathrm{i}\phi}$. If we choose F and G to be smooth functions and $F\to0$ and $G\to1$ as $r\to\infty$ faster than $1/r^3$ and $1/r^2$, the coupling between the Floquet blocks will approach zero as $r\to\infty$ at least as fast as

$1/r^2$. For all of our applications, we have chosen functions of F and G that converge to their asymptotic forms as fast (or faster) than Gaussian functions of r. Therefore, we can use these functions to construct scattering-type wavefunctions that are well behaved near the origin and at large distances. This formulation *allows* a scattering-type treatment of multiphoton ionization using any of the standard methods utilized for scattering calculations (e.g. R-matrix, close coupling, Kohn variational principles, Schwinger variational principles).

Formally, the resulting S-matrix is independent of the particular choice of F and G as long as $F \to 0$ and $G \to 1$ as $r \to \infty$ sufficiently fast. To show the independence of the S-matrix, assume that you have two different choices of phase operators, $\phi^{(1)}$ and $\phi^{(2)}$, that satisfy the condition on F and G. With these two choices of phase operator there are two corresponding wavefunctions $\psi^{(1)}$ and $\psi^{(2)}$ which will give the same Ψ through (2); this is possible since Ψ is a solution of (1) which has no dependence on the phase operators. Equation (2) can be used to relate the two functions $\psi^{(1)}$ and $\psi^{(2)}$ to give

$$\psi^{(1)} = \exp(\mathrm{i}\phi^{(1)}) \exp(-\mathrm{i}\phi^{(2)}) \psi^{(2)} \tag{5}$$

since the phases are Hermitian. Both of the phase operators have the property that $F \to 0$ and $G \to 1$ as $r \to \infty$ which means $\phi^{(1)} \to \phi^{(2)}$ as $r \to \infty$ which means $\exp(\mathrm{i}\phi^{(1)}) \exp(-\mathrm{i}\phi^{(2)}) \to 1$ as $r \to \infty$. This shows that $\psi^{(1)} \to \psi^{(2)}$ as $r \to \infty$ and therefore the S-matrix must be independent of the choice of phase as long as $F \to 0$ and $G \to 1$ as $r \to \infty$. A test of the accuracy of calculations with a mixed gauge can be obtained through a comparison of physical parameters (such as the S-matrix) for different choices of F and G.

The $\psi_{Ej}(\boldsymbol{r}, t)$ is a solution of the equation

$$E\psi_{Ej}(\boldsymbol{r}, t) = (\tilde{H} - \boldsymbol{A}(t) \cdot \boldsymbol{A}(t)/2c^2)\psi_{Ej}(\boldsymbol{r}, t) \tag{6}$$

where $\tilde{H} = \mathrm{e}^{\mathrm{i}\phi} H \mathrm{e}^{-\mathrm{i}\phi} - \partial\phi/\partial t - \mathrm{i}\partial/\partial t$; this equation is exact only when $[\phi, \partial\phi/\partial t] = 0$. The operator $\tilde{H}$ can be expressed in series form as

$$\tilde{H} = H - \frac{\partial\phi}{\partial t} - \mathrm{i}\frac{\partial}{\partial t} + \frac{1}{1!}[\mathrm{i}\phi, H] + \frac{1}{2!}[\mathrm{i}\phi, [\mathrm{i}\phi, H]] + \cdots \tag{7}$$

where the relationship from (4) has been utilized. With the mixed gauge transformations, these terms become very complicated which has some drawbacks for practical calculations. However, we have found that the F and G can be chosen so that only the terms explicitly written in (6) are needed for converged results. Often, the $[\mathrm{i}\phi, [\mathrm{i}\phi, H]]$ term can be ignored. The fast convergence results from the smoothness of F and G. If the F and G are substantially changing over a distance s, then the nth commutator has a rough magnitude of $|\boldsymbol{A}|/(s \cdot c \cdot \omega)$ where $|\boldsymbol{A}|/(c \cdot \omega)$ is the amplitude of oscillation of a free electron in a laser field. The rapidity of convergence can be increased by making s large (i.e. making F and G smoother).

The loose constraints on possible choices of ϕ is a powerful tool that can be used to allow different types of scattering calculations. For example, we always choose the phase operator in such a way that we can use R-matrix methods for the calculation. The conditions on ϕ are that at the R-matrix boundary F, $1 - G$ and $\mathrm{d}G/\mathrm{d}r$ are negligibly small at $r = r_0$. These conditions imply that ϕ gives the velocity-to-acceleration gauge transformation within negligible errors.

3. One-dimensional application

In order to investigate the usefulness and the convergence properties of the mixed gauge treatment, we have calculated decay rates of the ground state of a model one-dimensional

system. For the Floquet treatment of the model problem, we did not find it necessary to include the velocity-to-length mixed gauge transformation; i.e. we chose $F = 0$. The $\bar{H}$ operator can be found term by term with this choice of F. The first term

$$H - \frac{\partial \phi}{\partial t} - \boldsymbol{A} \cdot \boldsymbol{A}/2c^2 = \frac{p^2}{2} + V(x) + \frac{1}{2c}[(1-G)p + p(1-G)]A_0 \sin \omega t \tag{8}$$

is a Hermitian operator even when expanded in an R-matrix basis if $G = 1$ at the boundary. The second term

$$[\mathrm{i}\phi, H] = \frac{A_0}{\omega c} \cos \omega t \left[(p^2 G' + G' p^2 + 2pG'p)/4 + (pG' + G'p)\frac{A_0}{2c} \sin \omega t - G\frac{\mathrm{d}V}{\mathrm{d}x} \right] \tag{9}$$

(where $G' = \mathrm{d}G/\mathrm{d}x$) is also Hermitian when expanded in a R-matrix basis if $G' = 0$ at the boundary. The next-order term did not make a large contribution when G was a slowly varying function of position; the third term had a 1–2% effect on the branching ratios for the highest field strengths that were attempted with different choices of G. Note, that a pure velocity-to-acceleration gauge transformation ($G = 1$) would only give the term proportional to $\mathrm{d}V/\mathrm{d}x$. This term would cause difficult problems if the potential were singular. With the mixed gauge transformation, the G can be chosen so that $G\mathrm{d}V/\mathrm{d}x \to 0$ at any singularity. It is somewhat tedious to evaluate the next higher term. We have evaluated this term explicitly only for the length-to-velocity mixed gauge transformation. When we use the R-matrix technique to solve for the wavefunction, we use an approximation

$$\begin{aligned} \langle y_j | [\mathrm{i}\phi, [\mathrm{i}\phi, H]] | y_{j'} \rangle &= \langle y_j | \mathrm{i}\phi(p^\dagger, x, t)[\mathrm{i}\phi, H] - [\mathrm{i}\phi, H]\mathrm{i}\phi(p, x, t) | y_{j'} \rangle \\ &\simeq \sum_{j''} \{ \langle y_j | \mathrm{i}\phi(p^\dagger, x, t) | y_{j''} \rangle \langle y_{j''} | [\mathrm{i}\phi, H] | y_{j'} \rangle \\ &\quad - \langle y_j | [\mathrm{i}\phi, H] | y_{j''} \rangle \langle y_{j''} | \mathrm{i}\phi(p, x, t) | y_{j'} \rangle \} \end{aligned} \tag{10}$$

where $p^\dagger$ means $\mathrm{i}\partial/\partial x$ acting to the left. (The first equivalence only holds when $[\mathrm{i}\phi, H]$ is zero at the R-matrix boundary; the G can be chosen so that G' is arbitrarily small at the boundary but V' may not be small. When $V' \neq 0$ at the boundary, a surface term needs to be included in the first line of (10).) By writing this matrix element as a matrix multiplication, we are saved the problem of explicitly evaluating many new integrals. We have found that this approximation gives good results for the one-dimensional problem that we have examined. Repeating the matrix multiplication to get higher-order terms gives inferior results. We did not obtain good results when $p^\dagger$ was replaced by p because the matrix multiplication did not converge rapidly with basis size; the matrix elements do not converge quickly when the momentum operator acts on the basis function that is being summed. All of these statements are based on an examination of the independence of physical parameters as the phase operator was changed.

An examination of the terms in (8)–(10) would show that the interaction between the different Floquet blocks converges asymptotically to zero like $\mathrm{d}V/\mathrm{d}x$. For the three-dimensional hydrogen atom, this derivative of the potential would go to zero like $1/r^2$. The fast convergence of the coupling to zero allows the calculation of scattering-type functions without any additional transformations. We construct the wavefunction ψ_{Ej} using a Floquet expansion

$$\psi_{Ej}(x, t) = \sum_{j'} \exp(-\mathrm{i}\omega n_{j'} t)\psi_{Ej',j}(x) \tag{11}$$

where the $\psi_{Ej',j}(x)$ have the asymptotic form

$$\psi_{Ej',j}(x) = (f_{j'}^{+}(x)\delta_{j'j} - f_{j'}^{-}(x)S_{j'j})\mathrm{i}/\sqrt{2} \qquad |x| > x_0 \tag{12}$$

and the $f_{j'}^{\pm}$ are the solution of the unperturbed asymptotic equations at energy $\epsilon_{j'} = E + n_{j'}\omega$. For short-range potentials

$$f_{j'}^{\pm}(x) = \frac{1}{\sqrt{\pi k_{j'}}} \exp(\pm i k_{j'} x) \tag{13}$$

where $k_{j'} = \sqrt{2\epsilon_{j'}}$; when the potential is asymptotically Coulombic, $f_{j'}^{\pm} = c_{j'} \pm i s_{j'}$ (Seaton 1983) or equivalently $f_{j'}^{\pm} = (-g_{j'} \pm i f_{j'})/\sqrt{2}$ (Fano and Rau 1986) where $f_j(r)$ ($g_j(r)$) is the regular (irregular), energy-normalized Coulomb function of energy ϵ_j and angular momentum ℓ_j.

We solve for the $\psi_{Ej',j}$ using the variational R-matrix method (Greene 1985, Schneider 1975, Robicheaux 1991); we use the form of Schneider and Robicheaux for the calculations. In this method we expand the Hamiltonian in a basis, $Y_a(x,t) = y_{n_a}(x)\exp(-i n_a \omega t)$, that does not all have the same logarithmic derivative on the boundary. For all of our calculations we used two functions that had zero derivative on the boundary and the rest that went to zero on the boundary. In this basis, the R-matrix is

$$R_{j'j} = -\tfrac{1}{2} y_{j'a'} y_{ja} [(E - \bar{H} - L)^{-1}]_{aa'} \tag{14}$$

where $y_{ja} = \delta_{n_j n_a} y_{n_a}(x_0)$ and L is the Bloch operator. We choose G so the equations are transformed to the acceleration gauge at $x = x_0$; therefore, we do not need any further transformations outside of the R-matrix box.

We obtained the decay rate and branching ratios for the ground state by treating it as a resonance in a multichannel continuum. We utilized the delay-time formalism of Smith (1960) which uses the S-matrix at real energies to get the width and branching ratios of a resonance; Sadeghpour *et al* (1992) used this method to describe the resonant doubly excited states of H^-. In this formalism

$$Q = i\frac{dS}{dE} S^{\dagger} \tag{15}$$

is the Hermitian delay-time matrix. The largest eigenvalue of Q near a resonance has the Lorentzian form

$$q(E) = \Gamma/[(E - E_r)^2 + (\Gamma/2)^2] \tag{16}$$

where Γ is the full width of the resonance. To obtain Γ and E_r, we calculated the largest eigenvalue of Q at hundreds of energies and fit it to the form of (16). The branching ratio of the resonance to the channel j is given by the squared magnitude of the jth element of the eigenvector of Q for the largest eigenvalue at energy E_r.

As a test calculation, we found the decay rate of the ground state of the potential $V(x) = -\exp(-x^2)$ which has a ground-state energy of -0.4774 au. We converted the range $-\infty < x < \infty$ to $0 \leqslant x < \infty$ by forcing the parity of the n Floquet block to be $(-1)^n$. Calculations were performed for many different choices of ω and A_0. As a demonstration of the convergence properties of the method, we performed extensive calculations with the parameters $\omega = 0.2$ au and $A_0 = 63.3$ au. With this choice of parameters, three photons are needed to detach the electron. In the acceleration gauge, the amplitude of the oscillations of the potential is $A_0/c\omega \simeq 2.3$ au. We chose a mixing function $G(x) = (1 - \exp(-\beta(x - x_c)^4))\Theta(x - x_c)$ where $x_c = 2$ au and Θ is the Heaviside step function. This mixing function is smooth at the accuracy level of our calculations. The parameter β is chosen so that $1 - G(x_0) < 10^{-7}$ au where x_0 is the size of the R-matrix volume. In tables 1 and 2, we summarize the convergence of our calculation with the size of basis set and choices of parameters. For these tables, n_{lo} (n_{hi}) is the lowest (highest) Floquet block of basis functions in the calculation, N is the number of basis for each Floquet block,

Table 1. Convergence with Floquet blocks.

n_{lo}	n_{hi}	E_r (au)	Γ (au)	B_3	B_4	B_5	B_6	B_7
0	3	−0.516 1	2.99(−4)	1.00	0.00	0.00	0.00	0.00
0	4	−0.515 6	1.64(−4)	0.31	0.69	0.00	0.00	0.00
−1	4	−0.535 11	9.97(−4)	0.911	0.089	0.00	0.00	0.00
−1	5	−0.535 12	1.04(−3)	0.836	0.154	0.010	0.00	0.00
−2	5	*−0.536 504*	*1.127(−3)*	*0.848*	*0.143*	*0.009*	*0.00*	*0.00*
−2	6	−0.536 506	1.121(−3)	0.850	0.122	0.028	0.001	0.00
−3	6	−0.536 583	1.126(−3)	0.850	0.121	0.028	0.001	0.00
−2	7	−0.536 506	1.121(−3)	0.850	0.108	0.040	0.002	0.000
−2	8	−0.536 506	1.121(−3)	0.850	0.107	0.037	0.007	0.000
−2	9	*−0.536 506*	*1.121(−3)*	*0.850*	*0.107*	*0.036*	*0.007*	*0.000*

Table 2. Convergence with number of basis per channel.

N	E_r (au)	Γ (au)	B_3	B_4	B_5	B_6	B_7
24	−0.536 388	1.112(−3)	0.850	0.108	0.040	0.002	0.000
26	−0.536 453	1.117(−3)	0.850	0.108	0.040	0.002	0.000
28	−0.536 488	1.120(−3)	0.850	0.108	0.040	0.002	0.000
30	−0.536 506	1.121(−3)	0.850	0.108	0.040	0.002	0.000

E_r is the energy and Γ is the total width of the resonance, and B_n is the branching ratio for n photon detachment. The decay rate from a time-dependent calculation is $1.2 \pm 0.1 \times 10^{-3}$ au. The resonance energy has a substantial shift from the zero-field value of −0.4774 au.

In table 1 we explore the convergence properties as a function of the number of Floquet blocks included in the calculation. For all of the calculations in this table, $\beta = 3 \times 10^{-5}$ au, $x_0 = 30$ au, and $N = 30$. From this table, it is clear that the position and width of the resonance are converged at the 1% level using $n_{lo} = -2$ and $n_{hi} = 5$. Changing n_{hi} to 6 converges the branching ratios at the 1% level which is extremely fast since the $n = 6$ channel mixes in at the 1% level. At $n_{hi} = 7$, all of the parameters are converged at the 0.5% level. This behaviour is in contrast to calculations that matched different gauge wavefunctions at fixed distances (Grant and Greene 1994). In this matching calculation it was found that (for oscillations $A_0/c\omega < 1$ au) the number of Floquet blocks needed for convergence was 2–5 times the number of Floquet channels that were physically coupled. This slower convergence may be related to the abrupt matching; it is well known that abruptly changing functions are more difficult to represent with a basis than smoothly evolving functions. The Floquet expansion is a particular representation of the wavefunction which converges more or less quickly depending on the physical situation that is being described. In atomic R-matrix calculations, the limiting factor is the number of channels/Floquet blocks that can be included in a calculation. The fast convergence with Floquet blocks compensates for the additional work needed to calculate the Hamiltonian matrix elements.

In table 2, we have fixed $n_{lo} = -2$ and $n_{hi} = 7$ to study the convergence with the number of basis functions per channel. The branching ratios are converged at the 0.01% level and the total decay rate at the 1% level with 24 basis functions. It appears that for the calculations of Burke *et al* 50 basis functions per channel were needed for convergence at this level for similar frequency and field strengths.

As a final test of this method we increased the R-matrix box size to 34 au with 30 basis

Table 3. Convergence of the time-dependent decay rate with grid spacing for the four different gauges.

Δx	Length	Velocity	Mixed	Acceleration
0.1	2.78	2.78	2.79	2.79
0.2	2.74	2.74	2.77	2.81
0.4	2.58	2.58	2.72	2.90
0.6	2.34	2.35	2.66	2.97
0.8	2.16	2.18	2.73	2.64

functions per channel. We used $n_{lo} = -2$ and $n_{hi} = 7$. We found that changing β from 6×10^{-5} au to 1.5×10^{-5} au changed the resonance width by 0.1% and did not change the resonance position. The branching ratios to the three- and four-photon channels changed by 1%. For exact calculations, none of the physical parameters should change with β.

The majority of this section has focused on Floquet applications with a mixed gauge treatment of the laser field. We have chosen this emphasis because of our feeling that the time-independent methods have a stronger need for this gauge. However, it is not obvious that the standard gauges are better than a mixed gauge for time-dependent calculations. To demonstrate the possible superiority of the mixed gauge, it is *necessary* to show the mixed gauge calculations converge faster with Δx (the spatial grid spacing) or Δt (the time step) than the standard gauges. The more complicated mixed gauge Hamiltonian will cause the mixed gauge codes to be slower than the codes based on the standard gauges for the same number of spatial and temporal points.

To study time-dependent approaches, we used the length-to-velocity mixed gauge transformation in time-dependent codes

$$\Psi(x,t) = e^{-i\phi(x,t)}\psi(x,t) \tag{17}$$

where $\phi(x,t) = F(x)xA(t)/c$. The $\psi(x,t)$ is a solution of

$$i\frac{\partial\psi(x,t)}{\partial t} = \left\{\frac{1}{2}\left[p + \frac{A(t)}{c}(1 - F(x) - xF'(x))\right]^2 + V(x) - \frac{1}{c}\frac{dA(t)}{dt}xF(x)\right\}\psi(x,t) \tag{18}$$

where we choose $F(x) = \exp(-x^2/2)$. For the time-dependent calculations, we used $V(x) = -1/\sqrt{0.5 + x^2}$ for the static potential. For all of the gauges, the p^2 operator is evaluated using a three-point differencing method and the p operator is evaluated using a symmetric two-point differencing method. In the mixed gauge calculation, the $p(1-F(x)-xF'(x))\psi(x,t)$ term is evaluated by using a symmetric two-point differencing method for p; we do *not* replace this term with $[i(2F'(x) + xF''(x)) + (1 - F(x) - xF'(x))p]\psi(x,t)$ because this replacement would cause the discretized Hamiltonian to be non-Hermitian (the discretized mixed gauge Hamiltonian is exactly Hermitian without the replacement). We have added an absorbing potential at large distances to prevent reflection from the edge of the spatial grid; the absorbing potential was not necessary for the calculations we report because we stop the calculation well before the reflected wave would reach the origin. Our grid extends from -60 to 60 au. The laser has a $\sin^2(\omega t/20)$ turn-on over five laser periods.

In table 3, we show the decay rate for the ground state for the four different gauges as a function of the spatial grid spacing, Δx. For this table, $\omega = 1$ au and the steady intensity was 1.4×10^{15} W cm^{-2} = 2 au. At this frequency only one photon is needed to ionize the 'atom'. This table shows that the mixed and acceleration gauges have a comparable accuracy and both are much more accurate than the length and velocity gauges. For our

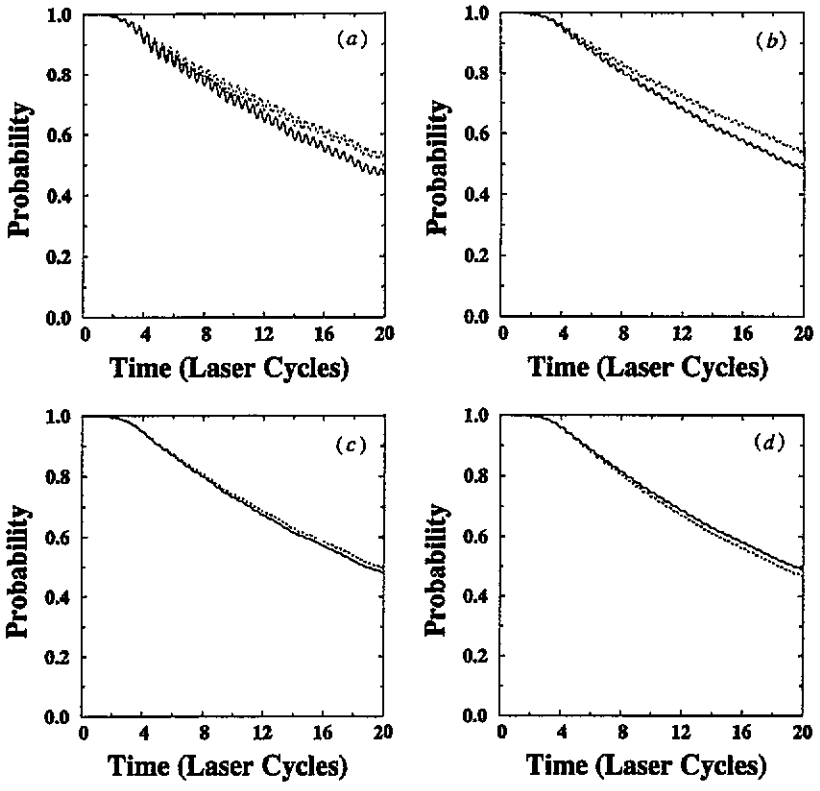

Figure 1. The time-dependent calculation of $|\langle\psi(t)|\psi(0)\rangle|^2$ for (*a*) length, (*b*) velocity, (*c*) mixed, and (*d*) acceleration gauges. The full curve is for grid spacing $\Delta x = 0.1$ au and the broken curve is for $\Delta x = 0.6$ au.

choice of parameters (which were in no way optimized to give good results for the mixed gauge), the mixed gauge obtains the same level of accuracy as the length and velocity gauges with a mesh 60% larger than those gauges. In figure 1, we plot the correlation function, $|\langle\psi(t=0)|\psi(t)\rangle|^2$ for the four different gauges for $\Delta x = 0.1$ au (full curve) and $\Delta x = 0.6$ au (broken curve). These plots clearly show the larger error in the length and velocity gauge calculations. The norm of the wavefunction deviates from 1 (indicating the wavepacket has hit the absorbing potential) after 18 laser cycles.

We also carried out calculations for $I = 3.0 \times 10^{14}$ W cm^{-2} and $\omega = 0.33$ au. For this calculation, the length gauge needed a time step at least twice as small as the other gauges to get results converged at a comparable level. The acceleration gauge had dramatically poorer convergence with Δx compared to the other three gauges. For this calculation, the velocity and mixed gauge converged faster overall. For the few calculations we completed for intense (but not super-strong) laser fields, the mixed gauge always converged as fast as the fastest converging of the standard gauges. Each of the standard gauges converged slowly for at least one of the test calculations.

Three-dimensional calculations never use the acceleration gauge when the potential has a Coulombic singularity because the interaction will look like a proton swinging back and forth. This causes relatively large numerical errors. To date, three-dimensional time-dependent calculations have been performed in the length or velocity gauge. Our results

for the one-dimensional time-dependent calculations indicate the possibility that a mixed gauge program may be much more computationally efficient than the length or velocity gauge (remember that at each time step you multiply a vector by a matrix which is an N^2 operation where N is proportional to $1/(\Delta x \Delta y \Delta z)$). Many three-dimensional programs utilize an expansion in spherical harmonics; the mixed gauge reduces the number of angular momenta that need to be included.

Another possible area for improving computational speed is through greater accuracy in Δt. The number of operations goes like $1/\Delta t$ for a fixed initial and final time. Because some of the behaviour of $\Psi(x, t)$ is analytically incorporated into the phase operator ϕ, it is probable that the $\psi(x, t)$ varies more slowly with time in the mixed gauge than in the length or velocity gauges. This would allow a larger Δt for the mixed gauge. We have not explored this issue in detail because there is not a large concern for increasing Δt in practical time-dependent calculations.

4. Three-dimensional hydrogen atom

The exceptional convergence of the mixed gauge wavefunction for the model one-dimensional problem demonstrates the possibilities of the mixed gauge wavefunctions. However, most problems of interest are three-dimensional and involve Coulomb singularities. In this section, we explore the application of mixed gauge wavefunctions to the three-dimensional hydrogen atom. This will allow an honest evaluation of the difficulties and promise of the mixed gauge treatment of multiphoton dynamics for Floquet wavefunctions.

Atomic hydrogen has been studied extensively with many methods and the previous results provide ready benchmarks for comparison with those of the present approach. However, the application of the mixed gauge method to the hydrogen atom in a laser field is simplified because there is only one electron. The main difficulty is to express the matrix elements of the Hamiltonian in a simplified form that is computationally accurate and efficient. Since the form of the Hamiltonian is complicated by the mixed gauge, we chose $F = 0$ in the phase operator in order to simplify the form of the matrix elements. For the calculations of this section, the laser field is linearly polarized in the $\hat{z}$-direction so that the magnetic quantum number is conserved during the ionization process. We choose the phase operator to have the form

$$\phi(r, p) = -[G(r)p_z + p_z G(r)]A_0 \cos \omega t/2c\omega \tag{19}$$

where $G(r) = [1 - \exp\{-\beta(r - r_c)^4\}]\Theta(r - r_c)$. With this choice of phase, the Hamiltonian is in the velocity gauge near the nucleus and in the acceleration gauge at large distances. The $\bar{H}$ operator is expanded according to (7) and gives the first term the same as (8) except p is replaced by p_z. The next term consists of three commutators

$$[\mathrm{i}\phi, H] = -\frac{A_0}{4c\omega}\cos\omega t[\mathrm{i}(p_z G + G p_z), p^2] - \frac{A_0}{2c\omega}\cos\omega t[\mathrm{i}(p_z G + G p_z), V]$$
$$-\mathrm{i}\frac{A_0^2}{4c^2\omega}\sin 2\omega t[(p_z G + G p_z), p_z] \tag{20}$$

in which the first two commutators connect angular momentum states l to $l \pm 1$ and the third connects l to $l \pm 2$ and l in an R-matrix basis. The function G is chosen so the first and third commutator of (20) are negligibly small at the R-matrix boundary. This is a useful property since the resulting Hamiltonian is then Hermitian within negligible errors. We utilize the R-matrix method to obtain the Floquet wavefunctions. The explicit expressions of the matrix elements for these operators are given in the appendix.

We have found that within moderate intensity, the next term in $\bar{H}$, $[i\phi, [i\phi, H]]$, can often be neglected. When this term is small but necessary, it can be approximated by matrix multiplication as we did in the one-dimensional example. As in (10), we replaced p_z by $p_z^\dagger$ in the first term of the matrix multiplication to avoid slow convergence with basis size. However, unlike the one-dimensional example with a *short*-range potential, a surface term emerges as a result of the non-vanishing of the derivative of the potential at the R-matrix boundary (i.e. $p_z \rightarrow p_z^\dagger +$ surface terms). This surface term, which is of the order of $1/r_0^2$, can be made negligibly small by choosing a relatively large r_0; r_0 is the size of the R-matrix box. In case a small r_0 is desired, the surface term,

$$\frac{A_0^2}{2c^2\omega^2}\int_S \cos^2\omega t \cos^2\theta G^2 V' Y_a(r,t)\; Y_b(r,t)\,\mathrm{d}S \tag{21}$$

where $Y_a(r,t) = y_a(r)Y_{l_a,m_a}(\theta,\phi)\exp(-in_a\omega t)$ is an R-matrix basis function, should be included in the $i\phi(p^\dagger)[i\phi, H]$ matrix element. This term is non-zero only when it is evaluated between two open-type basis with the angular momentum $l_a = l_b$ or $l_a = l_b \pm 2$.

We choose the function G so that the acceleration gauge has been fully turned on at the R-matrix surface. The electronic potential outside of the R-matrix volume is $V(r - \alpha(t))$, where the amplitude of the oscillation $\alpha(t) = A_0 \cos\omega t/c\omega$. The deviation of this potential from a Coulomb potential is propotional to $1/r^2$ and the amplitude is less than 2 au at the intensity we examined. The R-matrix provides the multichannel analogue of the logarithmic derivative at the surface of the enclosed volume and includes all of the electron interactions inside of the volume. We find the asymptotic wavefunction by matching the linearly independent solutions of Schrödinger's equation outside the R-matrix volume. We chose a relatively large r_0 and expressed the solutions of the Schrödinger's equation as perturbative corrections to the Coulomb functions f and g; this includes most of the laser–atom interaction outside the R-matrix volume. This is analogous to a standard correction in the R-matrix treatment of electron–ion scattering. With $r_0 = 31$ au, the perturbative correction of the f and g functions outside the R-matrix boundary changes the decay rate and branching ratios by less than 1%. Interactions with the laser field outside of the R-matrix volume become more prominent if one reduces r_0.

In table 4 we test the convergence with Floquet blocks for the multiphoton ionization of the ground state of a hydrogen atom exposed to a laser field with frequency $\omega = 0.184$ au and intensity 1.3×10^{14} W cm^{-2} (the amplitude of the oscillation $A_0/c\omega = 1.80$ au). The branching ratios B_{nl} designates the probability the electron absorbs n photons into the angular momentum l channel. For this table we used $\beta = 3 \times 10^{-5}$ au, $r_0 = 31$ au, and $N = 30$, we obtained similar convergence properties to the one-dimensional example, with $n_{lo} = -2$ and $n_{hi} = 7$ giving converged results. As in the one-dimensional model calculation, the convergence is very rapid with the number of Floquet blocks; convergence

Table 4. Convergence with Floquet blocks for atomic hydrogen, $\omega = 0.184$ au.

n_{lo}	n_{hi}	E_r (au)	Γ (au)	B_{31}	B_{33}	B_{40}	B_{42}	B_{51}	B_{53}
0	5	−0.523 25	2.92(−3)	0.565	0.207	0.029	0.189	0.000	0.011
−1	5	−0.532 92	2.19(−3)	0.527	0.232	0.026	0.203	0.000	0.012
−2	5	−0.533 30	2.16(−3)	0.525	0.232	0.026	0.204	0.000	0.012
−3	5	−0.533 31	2.16(−3)	0.525	0.232	0.026	0.204	0.000	0.012
−2	6	−0.533 30	2.16(−3)	0.525	0.232	0.025	0.190	0.008	0.019
−2	7	−0.533 30	2.16(−3)	0.525	0.232	0.024	0.188	0.009	0.019
−2	8	−0.533 30	2.16(−3)	0.525	0.232	0.024	0.188	0.009	0.019

Table 5. Convergence with Floquet blocks for atomic hydrogen, $\omega = 0.65$ au.

n_{lo}	n_{hi}	E_r (au)	Γ (au)	B_{11}	B_{13}	B_{20}	B_{22}	B_{31}	B_{33}
0	3	−0.316	0.141	0.701	0.057	0.022	0.206	0.007	0.007
−1	3	−0.311	0.152	0.686	0.008	0.035	0.257	0.008	0.007
−2	3	−0.306	0.149	0.670	0.009	0.040	0.266	0.008	0.007
−3	3	−0.305	0.149	0.666	0.009	0.041	0.268	0.008	0.007
−4	3	−0.305	0.149	0.666	0.009	0.041	0.269	0.008	0.007
−3	4	−0.305	0.146	0.622	0.006	0.054	0.224	0.052	0.037
−3	5	−0.305	0.145	0.622	0.006	0.072	0.192	0.039	0.046
−3	6	−0.305	0.145	0.627	0.006	0.074	0.182	0.052	0.040
−3	7	−0.305	0.145	0.627	0.006	0.074	0.180	0.051	0.035

Table 6. Energies and decay rates for some selected states of atomic hydrogen, $\omega = 0.65$ au, intensity $= 7 \times 10^{15}$ W cm^{-2}.

State	Noble *et al* position	Decay rate	Present position	Decay rate
3s	−0.053 225 1	4.454(−3)	−0.053 196 6	4.5(−3)
3d	−0.055 966 4	9.890(−5)	−0.055 966 4	9.83(−5)
4s	−0.030 256 5	1.870(−3)	−0.030 249 1	1.88(−3)
4d	−0.031 427 5	5.442(−5)	−0.031 427 1	5.47(−5)
5s	−0.019 489 2	9.580(−4)	−0.019 481 6	9.4(−4)
5d	−0.020 092 1	3.084(−5)	−0.020 091 0	3.01(−5)

is obtained when the basis contains slightly more Floquet blocks than are physically coupled together. We calculated the same rates for $n_{lo} = -2$, $n_{hi} = 7$ and $\ell \leqslant 5$. The position and width of the resonance did not change at the 1% level. The only branching ratio that changed by more than 1% was B_{33} which decreased from 0.23 to 0.20 and B_{44} which increased from 0 (because the 4, 4 channel was not included in the calculation) to 0.03. The speed of the convergence with ℓ may be somewhat surprising for these high intensities. We stress that the fast convergence arises from explicit and analytic inclusion of some of the effects of the laser field into the mixed gauge transformation.

In table 5 we test the convergence with Floquet blocks for the multiphoton ionization of the ground state of a hydrogen atom exposed to a laser field with frequency $\omega = 0.65$ au and intensity 2.0×10^{16} W cm^{-2} ($A_0/c\omega = 1.79$ au); we used the same parameters as those in table 4 for the basis functions. We have seen that, in both cases, one can obtain decent results using ten Floquet blocks; each block contains two angular momentum states.

We have performed several calculations and compared the results with previous methods using the L^2 non-Hermitian Floquet formulation (Chu *et al* 1985) and the complex energy R-matrix Floquet method (Dörr *et al* 1993, Noble *et al* 1993). In table 6 we give some selected comparisons with the same truncated n and l as previous calculations. In the delay-time method for extracting resonance positions and widths, the decay rate is obtained by measuring the full width of $q(E)$ in (16). Quite often, especially in the multiphoton ionization of hydrogen, two or more resonances are close to each other so that the shape of the resonances deviates from the Lorentzian form. The numerical extraction of the width becomes somewhat ambiguous if the resonances are not well separated. An example is the 3d resonance located on the left wing of the 3s resonance and almost right at its half maximum. In ambiguous cases we have estimated the width by graphically measuring the full width at half maximum.

Most of the previous multiphoton ionization calculations of atomic hydrogen have focused on energy shifts and total decay rates of specific states. The branching ratios were rarely reported, probably due to the difficulty in obtaining these parameters. Using the delay-time formulation, the information of the branching ratios can be easily obtained. The most extensive report on the branching ratios of hydrogen atom was given by Dörr *et al* (1993). We explored extensively the ground state of the hydrogen atom in a laser field with frequency $\omega = 0.65$ au and $\omega = 0.184$ au, and compared the decay rate and branching ratios with figures given by Dörr *et al* (1993). In the two cases they report, we have agreement with their decay rates within 4% up to intensities of 2×10^{16} W cm^{-2} for $\omega = 0.65$ au, and up to 1.3×10^{14} W cm^{-2} for $\omega = 0.184$ au. Our branching ratios also follow their calculation within 2% except at intensities above 10^{14} W cm^{-2} for $\omega = 0.184$ au ($A_0/c\omega = 1.58$ au). For this frequency, their B_{42} passes its maximum around 1.1×10^{14} W cm^{-2} ($A_0/c\omega = 1.69$ au) while ours keeps increasing. Dörr *et al* (1993) also provided branching ratios using a Sturmian Floquet approach at intensity 10^{14} W cm^{-2}. The Sturmian Floquet approach gave $B_{42} \simeq 0.15$ while the R-matrix result by Dörr *et al* was 0.13. We have obtained $B_{42} = 0.148$ for this frequency and intensity which is very close to the Sturmian Floquet calculation.

5. Discussion

The mixed gauge treatment of non-perturbative laser–atom interactions is based on the obvious fact that there are an infinite number of possible gauges and the gauge can be chosen in order to analytically incorporate the correct asymptotic nature of the interaction. With the power of modern computers, it is not necessary to remain wedded to the three standard gauges. That we *can* choose a gauge that simplifies the numerical description of the wavefunction is proved by the fast convergence of the numerical wavefunction with the number of Floquet blocks. Furthermore, the simplicity of the idea should allow it to be easily incorporated into existing computer programs. An interesting prospect involves the fast convergence: is the convergence fast enough to allow accurate calculations for laser interactions with multielectron atoms?

The mixed gauge idea can be utilized in time-dependent calculations. We do not know whether it is *desirable* to use mixed gauges in time-dependent calculations in three dimensions. Our results on a one-dimensional model problem indicates there are positive aspects of mixed gauge time-dependent wavefunctions. These calculations demonstrate the fast convergence of the mixed gauge wavefunction with Δx (the spatial grid spacing). The more complicated Hamiltonian that is a signature of the mixed gauge will slow the time-dependent codes for a fixed Δx but the mixed gauge codes are often much faster than the length and ty codes for a fixed level of accuracy. The general phase operator describes a larger part of the wavefunction analytically in the mixed gauge. The numerical part of the wavefunction will then be much simpler (as it is in the Floquet calculations), thus reducing the number of spatial mesh points needed for the wavefunction (which increases the speed of the calculation). It is also possible that a mixed gauge would improve the stability of the time-dependent calculations or possibly allow larger time steps (the small number of Floquet blocks in the time-independent calculations indicates a slower time evolution of the numerical wavefunction for the mixed gauge). Even if the codes are slower with a mixed gauge, the resulting wavefunctions may be easier to interpret which could aid in the identification of decay mechanisms.

Our calculation of the mixed gauge Floquet wavefunction is firmly based on a scattering formalism. This formalism allows a simpler description of electron–ion or electron–atom

scattering than of the decay of bound states in a laser field. There are several interesting aspects of the exchange of photons with the laser field during the collision of an electron with an atom or ion. For example, is the exchange of photons enhanced as a function of the incident electron direction? Preliminary calculations show a strong dependence of the total scattering cross section with emission or absorption of n photons as a function of the incident angle for electron–Ar scattering in the field of a CO_2 laser. What are the systematic properties for electrons scattering from a proton and laser field? What are the systematic properties for electrons scattering from atoms and laser field?

A final possible use for the mixed gauge is for improved theoretical treatment of asymptotic field strengths. In the approximations developed by Keldysh (1965) and Reiss (1980), rates are obtained by projecting the acceleration gauge wavefunction with zero potential onto the initial function. It is possible that more accurate first-order terms may be obtained by utilizing a mixed gauge transformation for the zeroth-order wavefunctions. This possibility has not been explored.

We feel that the mixed gauge approach may be very useful in the theoretical treatment of laser atom interactions and merits more study. Most of the questions and possibilities raised in this paper will be addressed in the future.

Acknowledgments

FR acknowledges conversations with U Fano and CH Greene. FR and CTC are supported in part by an NSF Young Investigator grant (NSF-PHY-9457903) with Auburn University. PG and MSP are supported in part by an NSF grant (NSF-PHY-9122199) with Auburn University.

Appendix

Here we give some matrix elements of the mixed gauge Hamiltonian for a three-dimensional application. Let $Y_a(r,t) = y_a(r)Y_{l_a,m_a}(\theta,\phi)\exp(-in_a\omega t)$ be the basis function, we then obtain

$$\begin{aligned}\langle Y_a(r,t)|\frac{A_0}{2c}\sin\omega t\left[p_z^\dagger(1-G)+(1-G)p_z\right]|Y_b(r,t)\rangle \\ = -\frac{A_0}{4c}(\delta_{n_a+1,n_b}-\delta_{n_a,n_b+1})(-1)^{l_a-m_a}\begin{pmatrix} l_a & 1 & l_b \\ -m_a & 0 & m_b\end{pmatrix}\langle l_a\|C^{(1)}\|l_b\rangle \\ \times\int(1-G)\left[(y_a y_b'-y_a' y_b)+(l_b-l_a)(l_b+l_a+1)\frac{1}{r}y_a y_b\right]\mathrm{d}r \qquad \text{(A1)}\end{aligned}$$

where $C^{(1)}$ is the unit spherical tensor of rank 1 and $m_a = m_b$ as a result of the linear polarizability of the laser field.

$$\begin{aligned}\langle Y_a(r,t)|-\frac{A_0}{4c\omega}\cos\omega t\left[\mathrm{i}(p_z G+Gp_z),p^2\right]|Y_b(r,t)\rangle \\ = -\frac{A_0}{8c\omega}(\delta_{n_a+1,n_b}+\delta_{n_a,n_b+1})(-1)^{l_a-m_a}\begin{pmatrix} l_a & 1 & l_b \\ -m_a & 0 & m_b\end{pmatrix}\langle l_a\|C^{(1)}\|l_b\rangle \\ \times\int[-G''(y_a' y_b+y_a y_b')-4G' y_a' y_b' \\ +(l_b-l_a)(l_b+l_a+1)\frac{G'}{r}(y_a y_b'-y_a' y_b)]\,\mathrm{d}r \qquad \text{(A2)}\end{aligned}$$

$$\langle Y_a(\boldsymbol{r},t)| -\frac{A_0}{2c\omega}\cos\omega t\left[\mathrm{i}(p_zG+Gp_z),V\right]|Y_b(\boldsymbol{r},t)\rangle$$
$$= -\frac{A_0}{2c\omega}(\delta_{n_a+1,n_b}+\delta_{n_a,n_b+1})(-1)^{l_a-m_a}\begin{pmatrix} l_a & 1 & l_b \\ -m_a & 0 & m_b\end{pmatrix}\langle l_a\|C^{(1)}\|l_b\rangle$$
$$\times\int GV'y_ay_b\,\mathrm{d}r \tag{A3}$$

$$\langle Y_a(\boldsymbol{r},t)| -\mathrm{i}\frac{A_0^2}{4c^2\omega}\sin 2\omega t\left[(p_zG+Gp_z),p_z\right]|Y_b(\boldsymbol{r},t)\rangle$$
$$= -\frac{A_0^2}{8c^2\omega}(\delta_{n_a+2,n_b}-\delta_{n_a,n_b+2})$$
$$\times\left\{\left[\tfrac{1}{3}\delta_{l_a,l_b}+\tfrac{2}{3}(-1)^{l_a-m_a}\begin{pmatrix} l_a & 2 & l_b \\ -m_a & 0 & m_b\end{pmatrix}\langle l_a\|C^{(2)}\|l_b\rangle\right]\right.$$
$$\times\int G'(y_ay_b'-y_a'y_b)\mathrm{d}r$$
$$\left.+\delta_{l_>,l_<+2}\left[\frac{(l_b-l_a)}{2}\sqrt{\frac{((l_>-1)^2-\bar{m}^2)(l_>^2-\bar{m}^2)}{(2l_>-3)(2l_>+1)}}\right]\int\frac{G'}{r}y_ay_b\,\mathrm{d}r\right\} \tag{A4}$$

where $l_>$ is the greater of l_a and l_b.

If $\frac{1}{2\mathrm{i}}[\mathrm{i}\phi,[\mathrm{i}\phi,H]]$ in (7) is desired, one also needs the matrix elements of $\mathrm{i}\phi$

$$\langle Y_a(\boldsymbol{r},t)| -\mathrm{i}\frac{A_0}{2c\omega}\cos\omega t(p_zG+Gp_z)|Y_b(\boldsymbol{r},t)\rangle$$
$$= -\frac{A_0}{4c\omega}(\delta_{n_a+1,n_b}+\delta_{n_a,n_b+1})(-1)^{l_a-m_a}\begin{pmatrix} l_a & 1 & l_b \\ -m_a & 0 & m_b\end{pmatrix}\langle l_a\|C^{(1)}\|l_b\rangle$$
$$\times\left[Gy_ay_b|_{r_0}+\int G\left((y_ay_b'-y_a'y_b)+(l_b-l_a)(l_b+l_a+1)\frac{1}{r}y_ay_b\right)\mathrm{d}r\right]. \tag{A5}$$

References

Burke P G, Francken P and Joachain C J 1991 *J. Phys. B: At. Mol. Opt. Phys.* **24** 761

Chu S-I and Cooper J 1985 *Phys. Rev.* A **32** 2769

Collins L A and Csanak G 1991 *Phys. Rev.* A **44** R5343

Collins L A and Merts A 1989 *Phys. Rev.* A **40** 4127

Dimou L and Faisal F H M 1994 *J. Phys. B: At. Mol. Opt. Phys.* **27** L333

Dörr M, Burke P G, Joachain C J, Purvis J and Terao-Dunseath M 1993 *J. Phys. B: At. Mol. Opt. Phys.* **26** L275

Dörr M, Joachain C J, Potvliege R M and Vucic S 1994 *Phys. Rev.* A **49** 4852

Dörr M, Terao-Dunseath M, Purvis J, Noble C S, Burke P G and Joachain C J 1992 *J. Phys. B: At. Mol. Opt. Phys.* **25** 2809

Fano U and Rau A R P 1986 *Atomic Collisions and Spectra* (Orlando, CA: Academic)

Giusti-Suzor A and Zoller P 1987 *Phys. Rev.* A **36** 5178

Grant A and Greene C H 1994 Private communication

Greene C H 1985 *Phys. Rev.* A **32** 1880

Grobe R and Eberly J H 1993 *Phys. Rev.* A **48** 4664

Keldysh L 1965 *JETP* **20** 1307

Krause J L, Schafer K J and Kulander K C 1992 *Phys. Rev.* A **45** 4998

Kulander K 1988 *Phys. Rev.* A **38** 778

LaGattuta K J 1991 *Phys. Rev.* A **43** 5157

Madajczyk J L, Pont M, Potvliege R M, Shakeshaft R and Taylor H S 1992 *Phys. Rev.* A **45** 4848

Maquet A, Chu S I, and Reinhardt W P 1983 *Phys. Rev.* A **27** 2946

Marte P and Zoller P 1991 *Phys. Rev.* A **43** 1512

Noble C J, Dörr M and Burke P G 1993 *J. Phys. B: At. Mol. Opt. Phys.* **26** 2983
Pindzola M S and Bottcher C 1993 *Laser Phys.* **3** 748
Pont M, Potvliege R M, Shakeshaft R and Teng Z-j 1992 *Phys. Rev.* A **45** 8235
Pont M, Shakeshaft R, and Potvliege R M 1990 *Phys. Rev.* A **42** 6969
Potvliege R M and Shakeshaft R 1989 *Phys. Rev.* A **40** 3061
Potvliege R M and Smith P H G 1993 *Phys. Rev.* A **48** R46
Reiss H 1980 *Phys. Rev.* A **22** 1786
Robicheaux F 1991 *Phys. Rev.* A **43** 5946
Sadeghpour H R, Greene C H and Cavagnero M 1992 *Phys. Rev.* A **45** 1587
Schneider B I 1975 *Chem. Phys. Lett.* **31** 237
Schwengelbeck U and Faisal F H M 1994 *Phys. Rev.* A **50** 632
Seaton M J 1983 *Rep. Prog. Phys.* **46** 167
Smith F T 1960 *Phys. Rev.* **118** 349
Xu H, Tang X and Lambropoulos P 1992 *Phys. Rev.* A **46** R2225